Ion mobility in α-PbF_2: a computer simulation study

2001 J. Phys.: Condens. Matter 13 51

(http://iopscience.iop.org/0953-8984/13/1/306)

INSTITUTE OF PHYSICS PUBLISHING JOURNAL OF PHYSICS: CONDENSED MATTER

J. Phys.: Condens. Matter **13** (2001) 51–66 www.iop.org/Journals/cm PII: S0953-8984(01)16287-9

Ion mobility in α-PbF_2: a computer simulation study

Michael J Castiglione[1], Mark Wilson[1], Paul A Madden[1] and Clare P Grey[2]

[1] Physical and Theoretical Chemistry Laboratory, Oxford University, South Parks Road, Oxford OX1 3QZ, UK
[2] State University of New York, Department of Chemistry, Stony Brook, NY 11794-3400, USA

Received 11 August 2000, in final form 1 November 2000

Abstract

Computer simulation studies of the F^--ion motion in pure and KF-doped α-PbF_2 are described. The aliovalent doping introduces vacancies into the crystal lattice which promote a significant degree of ionic motion, as witnessed by nuclear magnetic resonance and conductivity measurements. The simulations, using polarizable ionic potentials that have already been shown to reproduce the properties of the superionic conducting β-phase of PbF_2, give results which are consistent with these experimental data. A detailed site-hopping analysis is used to clarify the mechanism of the vacancy-promoted ionic motion, which differs markedly from the mechanism responsible for the facile ion diffusion in the β-phase.

1. Introduction

Lead (II) fluoride is one of a number of systems of stoichiometry MX_2 which exhibit fast-ion conduction. Of the single-cation halides supporting this property, PbF_2 has by far the lowest temperature of transition to the superionic state and, as a result, has attracted significant attention as a solid-state conductor [1]. The superionic form of PbF_2 has the cubic fluorite (β-) structure, but under a pressure of only 0.5 GPa [2] this phase undergoes a transition to a more closely packed cotunnite ($PbCl_2$ structure), denoted α. The α-phase is not superionic [2] (certainly not in the temperature range in which the β-phase already exhibits high conduction). However, NMR studies [3] indicate that there is some F^- intersite motion even at low temperatures, and show that this is enhanced in the presence of dopants, like KF [3–5], consistent with an anion vacancy mechanism for the diffusion. Probing the difference between the ion motion in the two phases should improve our understanding of the mechanism of the superionicity in the fluorite structure. The similarity of the energetics of the non-conducting α- and β-phases at close to room temperature and atmospheric pressure means that the two phases may be readily interconverted during preparation or processing, hindering the technological application of lead fluoride as a solid-state ionic conductor. We have already studied β-PbF_2 by computer simulation [6], developing an ionic potential from first-principles considerations based on electronic structure calculations on the in-crystal ions [7–9], and accurately reproducing many of the observed properties. In that work, we strongly emphasized

the role played by the large polarizability ($\alpha_{Pb^{2+}} = 17.9$ au) of the Pb^{2+} cation in the distinctive properties of lead fluoride. This arises from the $6s^2$ outer-electron configuration of Pb^{2+} which allows for relatively low-energy, dipole-allowed ns $\longrightarrow$ np transitions. Relative to that of a fluorite-structured alkaline-earth halide of the same cation size (SrF_2 or BaF_2), the higher polarizability ($\alpha_{Sr^{2+}} = 5.2$ au) enhances the F^- mobility in the β-phase (and also accounts for a distinctive difference in shape of the phonon dispersion relations [10–12]). However, the polarizability also contributes to lowering the pressure of transition to the α-phase relative to those of the alkaline earths.

The purpose of the present paper is to study the F^- motion in the α-phase with, and without, KF dopant. Initially, the objective will be to make contact with the experimental information by showing that the simulations (with the same potential as used for the β-phase study) predict a much lower degree of ionic motion in the α-phase relative to the β-phase at the same temperature; that the ion motion is greatly enhanced by the addition of small amounts of KF; and that the ion hopping is principally between type-1 and type-2 sites (see below), as demonstrated by the NMR experiments. We will then examine in detail the mechanism of ionic motion in the KF-doped systems in order to achieve an understanding of its relationship to that of the β-phase and to try to explain why the doped samples appear 'dynamically heterogeneous' [13, 14] in the NMR experiments—with sets of mobile and immobile F^- ions which remain distinct on long timescales.

2. Background information

2.1. The cotunnite structure

A projection of the cotunnite structure down the c-axis is shown in figure 1(a). The coordination environment about the cation is highly asymmetric, unlike the fluorite structure in which the cations sit in perfect (eight-coordinate) cubic sites in the simple cubic anion sublattice. There are seven 'short' Pb–F nearest-neighbour lengths between 2.41 Å and 2.69 Å and two 'long' lengths at 3.03 Å [2] (giving the quoted [7 + 2] coordination) compared with the fluorite Pb–F length of 2.56 Å [2]. Thus, although the mean bond length has increased from 2.56 Å to 2.66 Å, consistent with a phase transition to a higher-coordinate structure, there is a range of bond lengths, some of which are significantly shorter than in the low-pressure form.

In the context of the current work on F^- hopping, the structure is perhaps best approached in terms of the anion environment. There are two distinct fluoride sites: a four-coordinate (near-tetrahedral) site (termed type-1) and a five-coordinate site (termed type-2). Half of the sites of each type are occupied to form ordered sublattices. The two longer Pb–F bonds are associated with the type-2 sites. In the type-2 environment, the fluoride is located within an octahedral site, but displaced towards one of the vertices, such that the ion lies within a distorted square-based pyramidal site, leaving a vacant site on the other side of the octahedron. Any octahedral hole potentially gives rise to two such sites. The distance between the two sites is only 1.2 Å, which is far too short for both sites to be occupied simultaneously without substantial distortion of the octahedron. The vacant type-1 and type-2 sites will be denoted type-1′ and type-2′. The pattern of occupancy of the sites in the ideal crystal structure is illustrated in figures 1(b) and 1(c). The occupied square-based pyramidal (type-2) site shares triangular faces with three unoccupied tetrahedral (type-1′) sites and one unoccupied type-2′ site, as well as sharing its square face with another unoccupied type-2′, whereas the unoccupied type-2′ shares triangular faces with three type-1 and one type-2. The occupied tetrahedral type-1 shares faces with three vacant type-2′ and one type-1′. Thus an occupied site always shares faces with empty sites; occupied sites share edges with other occupied sites. Examination of

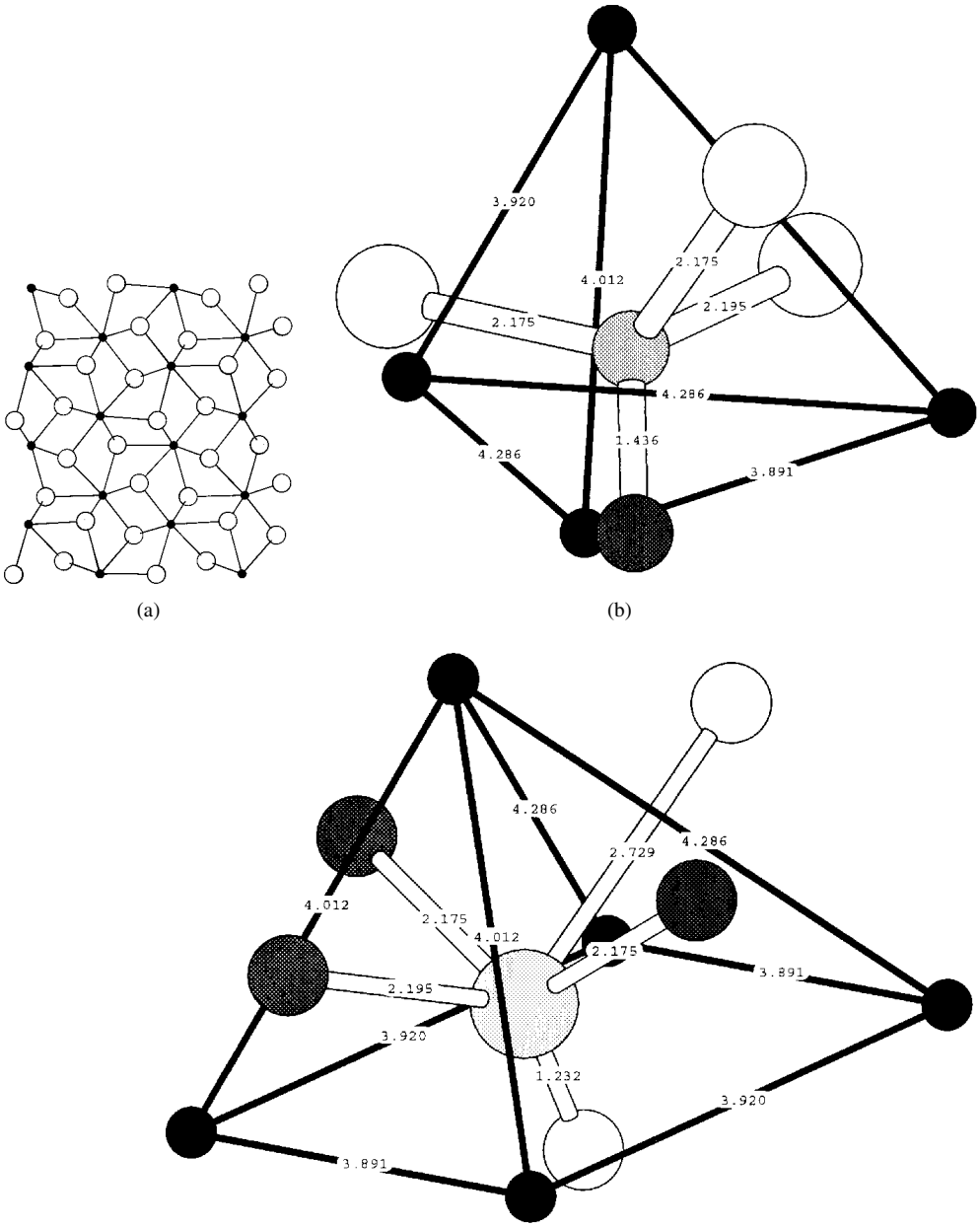

(a) (b)

(c)

Figure 1. (a) The cotunnite structure projected down the *c* axis—the small dark circles represent the Pb^{2+} ions, and the grey and white circles F^- ions in the type-1 and type-2 sites. (b) and (c) show the environment of the four-coordinate type-1 and five-coordinate type-2 sites, respectively, with the small dark circles representing Pb^{2+} ions. In both cases, the light grey circles are the occupied sites in the centres of their coordination polyhedra, and the white and dark grey circles are the locations of the closest unoccupied type-2′ and type-1′ sites.

the separation between the centres of sites that share faces shows that this is much smaller than the diameter of an F^- ion. Since each empty site is surrounded by four ions (for type-1′) and five (for type-2′) occupied sites, it seems extremely unlikely that these sites can be occupied unless this is accompanied by a substantial local deformation of the lattice.

It is of interest to contrast this picture of a lattice which has little free space to allow ionic motion with that pertaining to the β-phase. There, the F^- ions occupy tetrahedral sites which are adjacent to large, empty octahedral sites. It is believed that this space may contain an F^- ion, even if the adjacent tetrahedral sites remain occupied [15], and that it is this that permits the facile ionic conduction above the superionic transition temperature. By contrast in the α-phase, occupation of a site adjacent to an occupied type-1 or type-2 site appears unfavourable and intersite hopping is blocked when these sites are occupied. The existence of vacancies on the F^- sublattice appears to be necessary for fluoride-ion motion, and the creation of interstitials extremely unlikely.

2.2. NMR and conductivity results

The ^{19}F magic-angle spinning NMR spectra for pure α-PbF_2 exhibit two main resonances at room temperature. They are denoted F1 and F2 and assigned to the pseudo-tetrahedral, type-1 fluorides and the five-coordinate (type-2) fluorides, respectively. Above ∼400 K a third resonance appears at an average of the F1 and F2 resonance positions and arises as a result of fast exchange ($k > 28$ kHz or $t = 4 \times 10^{-5}$ s) between the two sites. Both the F1 and F2 resonances coexist with this line, and retain fine structure up to considerably higher temperatures. To explain this observation it is postulated that sets of 'mobile' and 'immobile' fluoride ions exist and remain distinct on very long timescales. The mobile ions undergo relatively frequent hops between type-1 and type-2 sites, so their contributions to the F1 and F2 lines collapse to form the central feature. 'Immobile' ions undergo some hopping (which may include 1–1 and 2–2 hopping), which causes incomplete collapse of the multiplet structure within the F1 and F2 lines. The increase of the intensity of the central resonance with increasing temperature is attributed to the increase in the proportion of the mobile ions. It has been suggested [3] that this 'dynamic heterogeneity' [13, 14] arises from increased mobility around intrinsic defects, which allow F^- vacancies to form in their vicinity, and essentially no motion in regions in which defects are absent. The proportion of mobile ions could increase with temperature because the number of such defects increases, but also because the volume of the mobile region around a defect increases.

Potassium-doped α-PbF_2 has also been studied [3]: at low concentrations, the K^+ ion is believed to occupy a normal cation site and therefore introduce a vacancy in the F^- sublattice; at higher concentrations new crystal structures are formed [5]. The doped form shows an increase in ion motion between type-1 and type-2 sites compared to the pure α-PbF_2. This is consistent with the vacancy-induced hopping mechanism. At doping levels of ∼0.5%, the distinction between 'mobile' and 'immobile' ions persists, so the additional vacancies do not allow hopping throughout the sample. 2-d NMR studies of the polarization transfer between mobile and immobile ions have confirmed that they remain distinct for at least 6×10^{-3} seconds at room temperature; this is an order of magnitude longer than the correlation time of the mobile ions. Only at doping levels of order ∼1% and at the highest observable temperatures (∼500 K) does the three-line NMR spectrum collapse to a single line.

Whilst there is clear NMR evidence for hopping of fluoride ions in the α-structure, it does not result in appreciable superionic conduction. In the pure α-phase the conductivity is only $5 \times 10^{-6}\ \Omega^{-1}\ cm^{-1}$ at 423 K, compared to $6 \times 10^{-5}\ \Omega^{-1}\ cm^{-1}$ for the β-phase [2, 16] at the same temperature, which is itself well below the superionic transition temperature of around

700 K. Above 700 K the β-phase conductivity increases rapidly with increasing temperature, as if some mechanism other than a vacancy- or interstitial-assisted hopping comes into play. In the α-phase, no comparable rapid increase occurs below 1000 K. Doping with K^+ promotes more hopping in the α-phase and increases the conductivity in proportion to the doping concentration, to a value of $\sim 5 \times 10^{-4}\ \Omega^{-1}\ cm^{-1}$ for a 0.5% solution at 423 K.

3. The simulations

3.1. Comparison of the NMR and simulation timescales

It is not possible to replicate directly the NMR observations in computer simulations because of the mismatch of timescales. As discussed above, at 473 K, about one quarter of the F^- ions in pure α-PbF_2 appear to participate in 1–2 hops, and the mean time between hops is of order 10^{-5} seconds. This means that in a simulation of the size of the one that we shall undertake, containing 648 ions (i.e. 432 F^-), we should wait of order 9×10^{-8} s between hopping events. To observe a significant number of events in a simulation of 0.1 ns, this time must be shorter by four orders of magnitude. Even this, however, presumes that the conditions necessary for hopping are present in the cell. If a pre-existing vacancy is required, this may not be so. In simulating pure α-PbF_2 we will be dealing with a perfectly pure system in which all the Pb^{2+} ions are vibrating about their lattice sites and in which periodic boundary conditions are enforced. In these circumstances, no vacancies are introduced, and their formation may be very slow. This problem will not be so pronounced in the KF-doped system, where vacancies *are* introduced, but even then the hopping rate at 473 K estimated from the NMR results is too slow for simulation. However, if we assume an activation energy for the hopping process in the doped sample of $\sim$35 kJ mol^{-1}, which is an average activation energy for the NMR correlation times calculated from data reported in [3] and [4], and agrees with that for the conductivity [16], then we may extrapolate from the NMR hopping time of $\sim 10^{-5}$ s at 393 K in a 0.2% solution to estimate that in a simulation cell of the above size where one vacancy is created by KF substitution (a 0.46% solution) we would see about 40 hopping events in a simulation lasting 0.1 ns at 800 K, and 100 at 900 K.

We shall, therefore, focus our simulations on this régime of elevated temperatures.

3.2. Simulation details

The simulation model for PbF_2 is based on a formal charge ionic effective pair potential (EPP) augmented with both anion and cation dipolar polarization effects. The short-range (overlap) parameters are fixed by fitting to *ab initio* calculations [7] that focus on the highly symmetric fluorite phase to allow the effective separation of the short-range and polarization terms. The polarizabilities are taken from additional *ab initio* calculations [7, 8] whilst the short-range contributions to the moments are derived from *ab initio* results for other fluorides using well-tested scaling arguments in terms of the ion radii [9].

The PbF_2 potential model has already been described in full in reference [6]. The additional terms required to describe the EPP for the interactions of the F^- and Pb^{2+} ions with K^+ are included in table 1. These parameters refer to a short-range repulsive potential of the form

$$u_{+-}^{EPP} = \frac{B_{ij}}{r_{ij}} e^{-a_{ij} r_{ij}} + B'_{ij} e^{-a'_{ij} r_{ij}^2} \tag{3.1}$$

between ions i and j. The dispersion parts of the pair potential include the long-range $C_6 r^{-6}$ (dipole–dipole) and $C_8 r^{-8}$ (dipole–quadrupole) terms, with r-dependencies modified at short range to account for dispersion damping [17]. The dispersion parameters C_6 and C_8

Table 1. Potential parameters for K^+–F^-, Pb^{2+}–K^+ and K^+–K^+ interactions.

Parameter	KF value (au)	PbK value (au)	KK value (au)
a	1.57	2.1447	0.0
a'	1.0	0.0	0.0
B	19.69	4613.6	0.0
B'	150000	0.0	0.0
C_6	0.0	53.045	0.0
C_8	0.0	711.042	0.0

are calculated from the in-crystal polarizabilities as discussed by Pyper [7] ($\alpha_{F^-} = 7.783$, $\alpha_{Pb^{2+}} = 17.9$ au and $\alpha_{K^+} = 5.4$ au respectively). The dispersion damping is described by Tang–Toennies functions (as in [18]), which contain a single parameter that specifies the length scale on which the damping becomes effective. In the present work the CaF_2 value of 2.9 is used [18].

All ions were treated as polarizable. The short-range induction damping parameters were assumed to be the same as for PbF_2, with $c_{-+} = 1.5$, $b_{-+} = 1.8$ and $c_{+-} = -0.3$ [6].

As predicted previously [6], the α-structure proved to be kinetically stable although slightly higher in energy with respect to the fluorite structure, in agreement with experiment [2].

Constant- (zero-) pressure MD runs were undertaken at several temperatures on pure α-PbF_2 systems containing 216 PbF_2 molecular units and on systems containing 215 Pb^{2+} ions, 431 F^- ions and a single K^+, which represent 0.46% KF–PbF_2 mixtures. The simulations were started from a perfect lattice, and an equilibration period of 10 ps was allowed before analysis was undertaken over a subsequent period of, typically, 240 ps. A density of 0.018 cations $Å^{-3}$ at 900 K was determined, which is similar to that expected from extrapolation of the experimental densities from lower temperatures.

3.3. Preliminary results

In figure 2 the mean square displacements of the F^- ions in pure α-PbF_2, pure β-PbF_2 and the 0.46% KF/α-PbF_2 mixture at the same temperature of 900 K are contrasted. The cations simply oscillate about their lattice sites in all three samples. It can be seen that the mobilities of the F^- ions in the two α-PbF_2 samples are *much* lower than in β-PbF_2 at this temperature (which is just above the superionic transition for the simulation potential). Even at this high temperature, very little anion motion is apparent in the pure α-PbF_2 system. Addition of the KF promotes some F^- motion, but considerably less than in the β-phase. At 950 K the mean diffusion coefficient of the 0.46% mixture is 1.9×10^{-7} cm^2 s^{-1} which may be compared with the simulation value for the pure β-phase at 950 K of 1.2×10^{-5} cm^2 s^{-1}. The simulations are therefore replicating, at least qualitatively, the effect of the phase change on the anion diffusion and the effect of the KF doping.

3.4. Hopping analysis

A central difficulty in analysing possible ion hopping mechanisms in computer simulations lies in the definition of whether or not a given ion lies within a given site. Often methods have defined a spherical region of space centred on the site, and considered any ion within that sphere to be contained within the site. The size of the sphere is somewhat arbitrary, and the approach

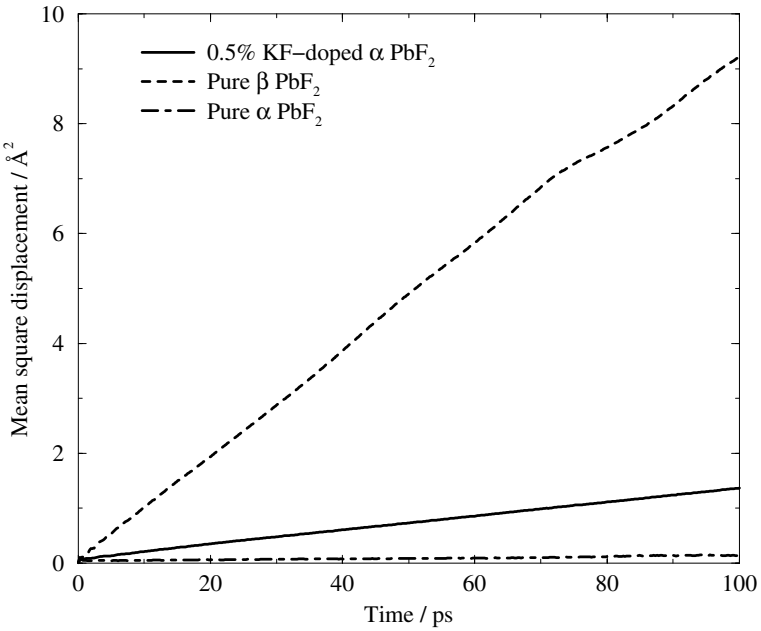

Figure 2. Fluoride-ion mean square displacements for pure and doped α-PbF_2 and pure β-PbF_2 at 900 K.

does lead to misassignments of ions to sites, and thus to an overcounting of hopping events. It is particularly unsatisfactory for asymmetrical sites such as the square-based pyramidal sites (type-2) in α-PbF_2.

A potentially more reliable method, where one sublattice retains a high degree of order, as with superionic conductors, is to use vector analysis to decide when an ion leaves a particular site polyhedron. As outlined in the discussion of the cotunnite structure, the space inside the crystal may be divided into tetrahedra and square-based pyramids whose vertices are at the positions of the Pb^{2+} ions of the ideal crystal. Since the Pb^{2+} ions do not change lattice positions in the course of the simulation, the identities of the ions at these vertices do not change. Fluoride ions may be assigned to these polyhedra in the initial structure, from the identities of the Pb^{2+} ions to which they are coordinated. In order to leave the polyhedron, an F^- ion must pass through one of its faces. Analysing this condition is simplified by noting that the polyhedral faces are triangular, or, in the square-base case, may be defined through two triangles that share a common edge. The condition of leaving the polyhedron may then be recast as finding when the scalar product of the ion's position vector, with respect to the position of one of the vertices of the triangle with a vector normal to the triangular plane, changes sign. Problems do arise for polyhedra with more than four faces, since in these cases certain triplets of vertices do not define external planes, so care must be taken to ensure that only the external planes are considered when calculating the scalar products. This requires additional code to pick out, for example, the internal planes in a 'square'-based pyramid.

Since the initial occupancy of each site is known from the start, and any hops that occur subsequently are recorded by the program, the positions of vacancies in the structure can be found from noting which type-1 or type-2 site becomes empty after one particular hop. By including the $1'$- and $2'$-sites in the analysis, the whole of space available to the fluorides is defined and thus the mechanism of motion can be investigated.

4. Analysis of the vacancy motion

As emphasized in the description of the cotunnite structure in section 2, occupation of interstitial (1′- and 2′-) sites whilst the adjacent 1- and 2-sites are occupied seems unlikely on geometrical grounds. This implies that ions cannot move through the lattice without the presence of vacancies on the type-1 and type-2 sublattices, and this appears to be consistent with the phenomenological observations.

We may use the hopping analysis described above to follow the ionic motion associated with the hopping of the vacancies introduced into the α-PbF_2 structure by KF doping by analysing the occupation of type-1 and type-2 sites. Notice that it is not sufficient simply to examine whether a site is occupied at a single instant in order to locate the vacancies. Since the type-1 and type-2 sites are bounded by (share all their faces with) empty type-1′ and type-2′ sites, ions may transiently leave a type-1 or type-2, even in the perfect crystal, in the course of their vibrational motion (see below). Including these events would lead to a substantial overcounting of vacancies. We therefore proceed by determining which ion is in each numbered type-1 or type-2 site in the initial crystal structure. This information is contained in an array, indexed by the ion label, whose elements are the site numbers, and also in a second array which is indexed by the site numbers whose elements are the ion numbers. In the case where one PbF_2 'molecule' has been replaced by one of KF, the latter would record the identity of the one empty site. As the molecular dynamics run progresses, the site analysis is conducted at regular intervals (typically separated by 0.1 ps) but the arrays are only updated when it is found that an ion has left one site *and entered* another type-1 or type-2 site, i.e. when the identity of the empty site changes. In this way the history of hopping events may be traced.

The hopping statistics were gathered over the 240 ps history of the simulations of the KF-doped samples at different temperatures. The number of events which involve hops between the different types of site (1–2, 2–1, 1–1 and 2–2 hops) was then recorded. The results are given in table 2. We also determined mean waiting times between hops of a given kind, which is useful for a detailed examination of the mechanism of the vacancy motion.

Table 2. Numbers of hops between normal sites in the simulations of KF-doped α-PbF_2 and the pure compound.

Temperature	$1 \rightarrow 1$ hops	$1 \rightarrow 2$ hops	$2 \rightarrow 1$ hops	$2 \rightarrow 2$ hops
750 K	5	37	37	0
800 K	13	38	38	1
850 K	12	48	48	2
900 K	17	75	75	8
950 K	18	81	81	5
800 K (pure)	0	0	0	0
900 K (pure)	2	4	3	0

4.1. Vacancy hopping and diffusion

We may compare the predictions of the F^- diffusion coefficient given by a simple theory of vacancy hopping [1] with the diffusion coefficient directly calculated from the long-time behaviour of the mean squared displacement of the ions found in the simulation runs. This involves the assumptions that an ion can only move over an appreciable distance if a vacancy moves in the opposite direction, and that successive vacancy hops are uncorrelated. The comparison should indicate whether the hopping analysis, and the assumption of uncorrelated

hops, gives a complete picture of the processes responsible for diffusion or whether other effects, such as participation of intrinsic vacancies, must be accounted for. The vacancy diffusion coefficient (D_{vac}) is related to the frequency of vacancy jumps (ω) and the intersite distance (l) by

$$D_{vac} = \frac{l^2\omega}{6}. \tag{4.1}$$

For l we take the nearest-neighbour F–F separation in the crystal ($\sim$3 Å) and determine ω from the total number of hops at each temperature. Values of D_{vac} obtained in this way are shown in table 3, together with the fluoride-ion diffusion coefficients, calculated from the long-time ($>$10 ps) slope of the mean square displacement versus time, and multiplied by the number of F^- ions in the cell. Reasonable agreement between the two values is found, although the D_{vac}-values are always higher. This probably indicates a tendency of the vacancy to hop back into the site which it left on the previous hop. Such an event would add two to the number of vacancy hops, but contribute nothing to the diffusivity as the hopping ion simply returns to its initial site. The reasonable agreement suggests that there is very little ionic motion without the intercession of the vacancy introduced by the KF doping.

Table 3. Diffusion coefficients calculated from the vacancy hops compared to those calculated from the fluoride-ion mean square displacements.

Temperature	D_{vac}/m^2 s^{-1}	$D_{F^-}n_{F^-}$/m^2 s^{-1}
750 K	5.13×10^{-9}	3.78×10^{-9}
850 K	7.14×10^{-9}	4.44×10^{-9}
950 K	1.20×10^{-8}	8.23×10^{-9}

This finding enables us to make contact with a measured quantity since, within the assumption of uncorrelated hops, we can estimate the conductivity from the vacancy diffusion coefficient [1]

$$\lambda = \frac{e^2\rho D_{vac}}{k_B T} \tag{4.2}$$

where e is the electronic charge and ρ the vacancy concentration (the reciprocal of the simulation cell volume). The results (shown in figure 3) may be compared with experimental data [16] for a doped α-PbF_2 sample with a similar concentration of KF (0.5%), and nominally pure material: the experimental data were obtained at a lower temperature than is accessible in the simulation and have been extrapolated by assuming Arrhenius behaviour. It seems from this comparison that the simulation is predicting a conductivity somewhat smaller than estimated by extrapolating the experimental observations. The apparent Arrhenius energy predicted from the simulations (slope of the plot $\sim$18 kJ mol^{-1}) is lower than that obtained in the experiment—$\sim$37 kJ mol^{-1} is quoted in reference [16]. Some decrease of the activation energy at the higher temperatures of the simulations, due to thermal expansion and the increased degree of vibrational excitation, seems likely. Note that the comparison with experiment rests on the assumption that there are no other extrinsic defects in the real material other than those induced by KF doping. The elemental analysis of the nominally pure, commercially available samples of PbF_2 suggests quite high impurity concentrations [19] and this is consistent with the much higher conductivities reported for 'pure' α-PbF_2 than we would obtain for the perfect crystal (see below). In the light of this, it is reassuring that the estimated simulation conductivity is *lower* than observed experimentally, despite the lower value of the activation energy.

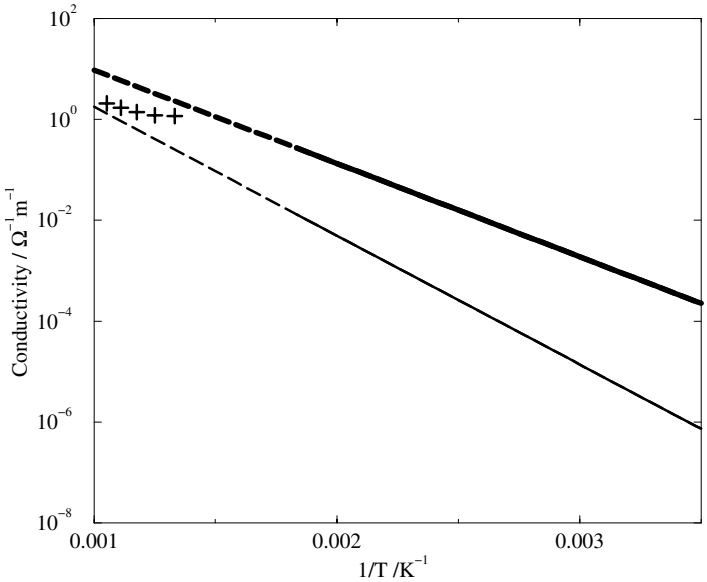

Figure 3. Conductivity calculated from D_{vac} from simulations (equation (4.2) compared to extrapolations of the Liang and Joshi experimental data for 0.5% KF-doped α-PbF_2 (thick line) and nominally pure α-PbF_2 (thin line). The solid lines reflect the actual experimental data and the dashed lines the Arrhenius extrapolations into the temperature régime of the simulations.

4.2. Vacancy hopping and NMR site exchange

The vacancy hopping characteristics found in the simulations are consistent with those of the 'mobile ion' NMR site exchange process. From table 2 it can be seen that the $1 \rightarrow 2$ and $2 \rightarrow 1$ hopping rates greatly exceed the rates of hopping between sites of the same type. Reasons for this will be discussed below. Thus, an ion's participation in the vacancy hops will lead to the collapse of the separate NMR resonances associated with the four- and five-coordinate sites, rather than to a collapse of the multiplet structure seen for each resonance (see section 2.2). The 'immobile' ions seen in the NMR experiments are those which have not participated in a vacancy hop, as the above considerations show that the ions do not move between sites without the intercession of a vacancy (the possibility of moving between occupied and interstitial sites will be considered below). The average activation energy for vacancy hopping of 25 kJ mol^{-1} is consistent with the activation energies calculated from the NMR exchange rates [3, 4] and NMR linewidths [20] for K^+-doped samples. (The difference between this activation energy and the one discussed above for the conductivity arises from the T^{-1}-factor in equation (4.2).) The observation of a smaller number of $1 \rightarrow 1$ hops in the simulations is consistent with NMR results. This was postulated in the previous study [3, 4] to explain the deviations in the intensities of the J-coupling multiplet of the F1 resonance at room temperature in comparison to the intensity predicted by a calculation that assumed a random distribution of ^{207}Pb spins.

A distinctive feature of the NMR observations is the long time associated with the exchange of mobile and immobile ions at temperatures up to 500 K, which suggests that (at the temperatures of the experiments) the vacancy is confined to a certain region of space, perhaps in the vicinity of the K^+ ions. For some samples, parts of the distributions of fluoride-ion correlation times can be ascribed to a heterogeneous distribution of the KF dopant throughout the samples, despite the efforts made to achieve uniformity in the synthesis. Nonetheless,

these results are still consistent with a localization of the vacancy near the defects. Visual examination of the migration pathway of the vacancy in the simulations does not suggest any strong tendency for localization around the K^+ site. In these circumstances, to make any statistically significant statement (independent of the starting configuration etc) we would have to allow the simulation to evolve until the number of hops exceeds the number of sites, and this is beyond our resources.

4.3. Vacancy energetics

By examining the waiting time between vacancy hops of different kinds, we may extract some information about the relative energies of the different sites occupied by the vacancy and about the activation energies of the pathways which connect them. If the hopping analysis shows that an ion makes (say) a $1 \rightarrow 2$ hop at some instant of time t_1, then we may deduce that the vacancy was on a 2-site immediately before t_1 and on a 1-site immediately afterwards. The next ion hop, at time t_2, must therefore be either a $2 \rightarrow 1$, in which case the vacancy has moved back to a 2-site, or a $1 \rightarrow 1$, when it remains on the type-1 sublattice but moves to a different 1-site. From the intervals between hops of particular types we may extract the fractions of the total simulation time, f_1 and f_2, that the vacancy spent on a type-1 or type-2 site. Values of these quantities at each temperature are shown in table 4: they show that the vacancy prefers to sit on the smaller, four-coordinate 1-site. The fractions should be proportional to the concentrations of vacancies which would be found on each type of site in a macroscopic sample, and hence their ratio should give a measure of the free-energy difference between the two sites through

$$\Delta G = -RT \ln \frac{f_1}{f_2}. \tag{4.3}$$

The data suggest a free-energy difference of $\sim$10 kJ mol^{-1} at 800 K. From an analysis of the temperature dependence of the ratio

$$\left(\frac{\partial \ln(f_1/f_2)}{\partial T} \right)_P = \frac{\Delta H}{RT^2} \tag{4.4}$$

we can separate an enthalpy difference of ~ -18 kJ mol^{-1} between vacancy occupation of the type-1 and type-2 sites.

Table 4. Fractions of time spent by the vacancy on type-1 and type-2 sites at different temperatures.

Temperature	f_1	f_2
750 K	0.843	0.157
800 K	0.817	0.183
850 K	0.792	0.208
900 K	0.742	0.258
950 K	0.759	0.241

If the vacancy is on a type-1 site it may hop to either a type-1 or a type-2 and the frequency of these events is determined by the numbers $n_{1\rightarrow1}$ and $n_{2\rightarrow1}$ of $1 \rightarrow 1$ and $2 \rightarrow 1$ *ion* hops (respectively) which are observed in the total simulation time τ of 240 ps (given in table 2). Since the vacancy is on a type-1 site for a time $f_1\tau$, rate constants for these events may be obtained from

$$k^v_{1\rightarrow1} = \frac{n_{1\rightarrow1}}{f_1\tau} \tag{4.5}$$

and

$$k^{v}_{1\to 2} = \frac{n_{2\to 1}}{f_1 \tau} \tag{4.6}$$

where the superscript v indicates that these are the rates of *vacancy* hopping, and similar expressions may be written for $k^{v}_{2\to 1}$. The number of $2 \to 2$ hops was always too low for a meaningful analysis to be applied. Values for these quantities are give in table 5 at different temperatures. From an Arrhenius analysis of the temperature dependence of these quantities we may obtain activation energies for the different pathways by which a vacancy can hop between sites. We obtain values of $E_A(1 \to 1) = 38$ kJ mol^{-1} for the less likely $1 \to 1$ hop, and values of $E_A(1 \to 2) = 30$ kJ mol^{-1} and $E_A(2 \to 1) = 12$ kJ mol^{-1} for the hopping between type-1 and type-2 sites. Note that the latter values are consistent with the enthalpy difference between vacancy occupation of the type-1 and type-2 sites evaluated above, and point to a significantly lower height for the barrier between these sites than between a pair of type-1 or type-2 sites. Very few hops between type-2 sites were seen in any of the simulations. The fact that the vacancy spends less time on the type-2 sublattice does affect this, but it seems that the $2 \to 2$ barrier is even higher than that between a pair of type-1 sites.

Table 5. Rate constants for hopping from a normal site to an interstitial.

Temperature	$k^{v}_{1\to 1}$/ps^{-1}	$k^{v}_{1\to 2}$/ps^{-1}	$k^{v}_{2\to 1}$/ps^{-1}
750 K	0.025	0.183	0.982
800 K	0.066	0.194	0.865
850 K	0.063	0.253	0.962
900 K	0.095	0.421	1.211
950 K	0.099	0.445	1.406

5. Involvement of the interstitial sites: vacancy hopping mechanism

As shown in figures 1(b), 1(c), the polyhedra surrounding the occupied type-1 and type-2 sites of the α-PbF_2 structure share faces only with the polyhedra of unoccupied sites and thus migration between type-1 and type-2 sites must necessarily be via a type-$1'$ or type-$2'$ site. It is of interest to see whether we can distinguish which of these migration pathways is preferred. Furthermore, we have so far excluded the possibility that an ion in a part of the lattice remote from a vacancy may enter such an interstitial site, i.e. that Frenkel pairs may play a significant role in the ionic motion. It is useful to try to elicit the energies, or timescales, associated with such a process relative to those involving a vacancy migration. In order to achieve this, the hopping analysis is generalized to include the primed sites. Note that this analysis is also applicable to pure α-PbF_2—without extrinsic vacancies—as well as the KF-doped systems.

We first consider the mechanism by which the $1 \to 1$ and $1 \to 2$ hops are accomplished in the KF-doped systems. The analysis described above allows us to isolate the time interval in which each vacancy hopping event occurs and identifies the ion which changes its lattice site during this interval. We may then track the movement of this ion during this interval in the generalized hopping analysis, recording which type of interstitial site it passes through. Note that this event (i.e. intersite ion hopping) *only* occurs in the presence of the vacancy on a neighbouring site.

The analysis shows that *all* of the $1 \to 1$ ion hops pass through a type-$2'$ site. Examination of the environment of each type of site in figures 1(b), 1(c) makes clear why this is so. A type-$1'$ site shares a common face with only one type-1 site (and three type-2); hence, a type-$1'$ site

cannot be a bridge between a pair of type-1 sites whereas a type-2′ can share faces with two type-1s and can thus provide a pathway between them. Note, however, that in this process, the extrinsic vacancy is on one of these type-1 sites and the ion making the hop originates from the other one, so the type-2 site which shares the octahedral hole with the type-2′ is still occupied. It seems likely that the repulsive interaction between the two ions within the octahedral hole will be quite strong (a typical distance between fluoride ions in F2 and F2′ is only 1.23 Å assuming no relaxation of nearby sites) and this may account for the relatively high value of the activation energy of the $1 \rightarrow 1$ pathway noted in the previous section.

On the other hand, geometrical considerations alone do not dictate the pathway for an ion hopping between neighbouring type-1 and type-2 sites; either a type-1′ or type-2′ might be involved. Examination of the trajectories shows, however, that at 800 K, ∼80% of the $1 \rightarrow 2$ ion hops pass through the type-1′ intermediate site, whereas for the reverse transition the proportion appears to be ∼65%. This is, perhaps, somewhat surprising. Since the forward hop starts with the extrinsic vacancy on a type-2 site, it might have been thought that the type-2′ site, with which it shares the octahedral hole, would have presented the most favourable transition state for the hopping ion. However, if one considers a hop from a type-1 site to a vacant type-2 site via a connecting 1′-site, the transition state involves an occupied 1′-site, which shares faces with two occupied type-2 sites and one vacant type-1 (the original site) and one vacant type-2 (the final site). There are thus no short 1′–1 distances (in the perfect crystal the distance between the sites is 1.44 Å), but there are two 1′–2 distances (2.17–2.20 Å in the perfect crystal). This situation (without accounting for relaxation) should result in less repulsion in the transition state than the alternative mechanism via a 2′-site, in which the transition state involves two 2′–1 contacts *together with* a 2′–2 contact at 2.73 Å. By a similar argument, type-2 → type-2 hops via a 2′-site are unlikely since the transition state involves *three* 2′–1 contacts, whilst a type-2 → type-2 hop via a 1′-site would involve a short 1′–1 contact.

To complete the examination of the role of the interstitial sites in the F^--ion motion, we return to the question of whether these sites may become occupied in the pure material, in the absence of any extrinsic vacancies. Such an excitation would comprise a Frenkel defect, with an unoccupied type-1 or type-2 site and the ion on an adjacent interstitial type-1′ or type-2′. To this end, we may contrast the total number of ion hops between occupied and interstitial sites observed in simulations of pure and KF-doped α-PbF_2 at the same temperature, system size and pressure. We analyse such data on the assumption that the doped system will exhibit a number of such hops in the vicinity of the vacancy *plus* a number of intrinsic hops and that the latter process will be the same as in the pure material.

A straightforward run of the site polyhedral analysis program records a large number of hops between occupied and interstitial sites. However, a large proportion of these are likely to be due to vibrational motion of the ions about their lattice sites at the high temperatures of the simulation. We therefore only record in the number of hops those cases where an ion is observed to move between sites in the interval (0.1 ps) between two analysis steps and where it does not hop back in the next interval. The recorded hops have therefore involved ion displacements which persist for at least 0.1 ps. In table 6 we give the data for the comparison between the pure and doped samples at two temperatures. The simulations contained 216 'molecules' and were run for 240 ps. We reiterate that no hops between occupied sites are seen in the pure material simulation at 800 K, although there is a small amount of hopping seen at 900 K (see below). It can be seen that the number of hops between occupied and interstitial sites is larger for the doped samples than for the pure material. We attribute this excess to the influence of the extrinsic vacancy. Occupied–interstitial hops induced by the vacancy may occur as part of the process of ion hopping between type-1 and type-2 sites, as discussed in

Table 6. Frequency of hopping from a normal site to an interstitial for the doped system compared to the pure compound.

Simulation	$1 \rightarrow 1'$	$1 \rightarrow 2'$	$2 \rightarrow 1'$	$2 \rightarrow 2'$
Pure, 800 K	40	6	0	24
Doped, 800 K	179	21	22	48
Pure, 900 K	306	31	3	106
Doped, 900 K	429	80	60	165

the previous section, i.e. they may be a part of a 'successful' ion move. Alternatively, the ion may simply drop back into its initial site, which could be called an 'unsuccessful' vacancy-assisted move. The remaining hops in the doped samples are presumed to arise at points in the lattice which are distant from the vacancy and to have the same properties and occur at the same rate as in the pure sample. We may therefore subtract the number of hops of each type found in the pure sample from the corresponding number for the doped one, to find the number of vacancy-assisted occupied–interstitial hops. Since we also know the number of ion hops between the type-1 and type-2 sites (section 4) and also the pathway taken during these hops (section 5) we may further calculate the number of vacancy-assisted occupied–interstitial hops associated with 'successful' ion moves. The full breakdown of the occupied–interstitial hops seen in the doped samples at 800 K and 900 K into intrinsic (transient Frenkel defect), and 'successful' and 'unsuccessful' vacancy-assisted hops is given in table 7. It can be seen that there are substantial differences between the success rates of different pathways, in the vacancy-assisted case. Note that the number of intrinsic hops is quite low at 800 K compared to the number of vacancy-assisted ones. It should be borne in mind that (almost) all the F^- ions in the lattice can participate in the former, whereas only those in the immediate vicinity of the vacancy can take part in the latter. The number of intrinsic hops (rate of Frenkel pair formation) increases with increasing temperature much more rapidly than the number of vacancy-assisted hops; it increases by a factor of 5–10 between 800 K and 900 K, depending on the type of hop involved. These values point to an activation energy of $\sim$100 kJ mol^{-1} (i.e. 1 eV) for this process, which seems like a reasonable value for the Frenkel pair formation energy at these high temperatures.

Table 7. Breakdown of normal $\rightarrow$ interstitial hops into vacancy, long-lived Frenkel defect and intrinsic non-vacancy mechanisms.

Type	$1 \rightarrow 1'_{800\,\mathrm{K}}$	$1 \rightarrow 1'_{900\,\mathrm{K}}$	$1 \rightarrow 2'_{800\,\mathrm{K}}$	$1 \rightarrow 2'_{900\,\mathrm{K}}$	$2 \rightarrow 1'_{800\,\mathrm{K}}$	$2 \rightarrow 1'_{900\,\mathrm{K}}$	$2 \rightarrow 2'_{800\,\mathrm{K}}$	$2 \rightarrow 2'_{900\,\mathrm{K}}$
Successful vacancy	20	39	12	54	19	57	9	20
Unsuccessful vacancy	119	84	3	0	3	10	23	39
Frenkel defect	40	305	6	27	0	1	24	105
Intrinsic	0	1	0	4	0	2	0	1

The rapid increase in the number of Frenkel pairs at high temperatures does allow the possibility of some ionic motion in the pure material, by hopping of the Frenkel pair. Values for the number of events in which ions exchange between type-1 or type-2 sites at 900 K are given in table 2. These numbers are small compared to the numbers occurring in the doped systems. It seems unlikely that such an event could be responsible for the ionic motion detected in the conductivity and NMR measurements on the 'pure' samples at lower temperatures, as the

activation energy $\sim$100 kJ mol^{-1} would be much larger than observed experimentally, whereas values comparable to the activation energy for the doped sample are reported (compare figure 3). It seems more likely that this motion is caused by vacancies introduced by impurities or at grain boundaries in the materials.

6. Conclusions

The combination of the insights emerging from the ^{19}F NMR studies and the present simulation work have allowed an examination of the mechanisms of ionic motion in doped and pure α-PbF_2 with unprecedented detail. The 'polarizable-ion' simulation model seems to have reproduced very satisfactorily the experimental observations on these materials, as well as on the superionic β-phase [6]. The agreement of NMR exchange rates, conductivities etc is not, in general, quantitative but this may be explained, in part, by the non-overlapping temperature ranges in which simulations and experiments were undertaken and by the very important role which might be played by defects in the real material, other than those introduced by aliovalent doping. α-PbF_2 emerges as a very useful material on which to study extrinsic vacancy hopping and its role in ionic conduction. The geometry of the cotunnite structure does not seem to permit the occupation of an interstitial site unless it is adjacent to a vacancy. Hence the spontaneous formation of unbound Frenkel pairs is suppressed and extrinsic vacancies dominate all observable characteristics of the ion motion up to very high temperatures. The lack of occupied interstitial sites is consistent with the NMR study where only normal and mobile sites were detected. Furthermore, low levels of potassium doping do not result in the formation of localized clusters or significant distortions in the surrounding lattice, again confirming the NMR results where no noticeable changes in ^{19}F chemical shifts were observed. We have been able to detail the migration pathways and the associated energetics of these vacancies. We have not been able to cast light on whether the vacancies are trapped in some extended neighbourhood of the introduced K^+ ions. Trapping of the vacancies in certain regions of the crystal appears to be indicated by the NMR observation that mobile and immobile ions only exchange on very long timescales. To examine such questions would involve very large-scale simulations.

This work clears the way for a simulation study of MF/PbF_2 mixtures at higher concentrations, where interesting new phases emerge [2]. We also plan to contrast the mechanism of ion motion in β-PbF_2 with that which has emerged in the present work.

Acknowledgments

We are grateful to Steve Hull for stimulating discussions and for sending data. MW thanks the Royal Society for a fellowship and MJC the EPSRC for a studentship. The work was supported by EPSRC grant GR/L/49369 and NATO grant CRG972228. CPG thanks the NSF for support (DMR-9901308 and DMR-0074858). Most of the simulations described in this paper were performed at the Oxford Supercomputing Centre.

References

[1] Chandra S 1981 *Superionic Solids. Principles and Applications* (Amsterdam: North-Holland)
[2] Hull S and Keen D A 1998 *Phys. Rev.* B **58** 14 837
[3] Grey C P and Wang F 1995 *J. Am. Chem. Soc.* **117** 6637
[4] Wang F and Grey C P 1998 *J. Am. Chem. Soc.* **120** 970
[5] Hull S, Berastegui P, Eriksson S G and Gardner N J G 1998 *J. Phys.: Condens. Matter* **10** 8429

[6] Castiglione M J, Wilson M, Madden P A and Pyper N C 1999 *J. Phys.: Condens. Matter* **11** 9009
[7] Pyper N C 1986 *Phil. Trans. R. Soc.* A **320** 107
[8] Pyper N C 1991 *Adv. Solid-State Chem.* **2** 223
[9] Ďemmer P, Fowler P W, Wilson M and Madden P A 1999 *J. Chem. Phys.* **111** 2038
[10] Dickens M H and Hutchings M T 1978 *J. Phys. C: Solid State Phys.* **11** 461
[11] Elcombe M M 1972 *J. Phys. C.: Solid State Phys.* **5** 2702
[12] Hurrell J P and Minkiewicz V J 1970 *Solid State Commun.* **8** 463
[13] Hurley M M and Harrowell P 1995 *Phys. Rev.* E **52** 1694
[14] Donati C, Glotzer S C and Poole P H 1999 *Phys. Rev. Lett.* **82** 5064
[15] Gillan M J and Dixon M 1980 *J. Phys. C: Solid State Phys.* **13** 1901
[16] Liang C C and Joshi A V 1975 *J. Electrochem. Soc.* **122** 466
[17] Stone A J 1996 *The Theory of Intermolecular Forces* (Oxford: Clarendon)
[18] Wilson N T, Wilson M, Madden P A and Pyper N C 1996 *J. Chem. Phys.* **105** 11 209
[19] Wang F 1998 *PhD Thesis* SUNY, Stony Brook
[20] Mahajan M and Rao B D N 1971 *Chem. Phys. Lett.* **10** 29